

# Estimation of harmonic impedance and resonance in power systems

Haitham Ali Alashaary<sup>1</sup>, Ghadeer Nyazi Al Shaba'an<sup>2</sup>, Wael Fawzi Abu Shehab<sup>3</sup>,  
Shehab Abdulwadood Ali<sup>4</sup>

<sup>1</sup>Department of Computer Engineering, Faculty of Engineering, Al-Hussein Bin Talal University, Maan, Jordan

<sup>2</sup>Department of Electrical Engineering, Faculty of Engineering, Al-Balqa Applied University, Al-Salt, Jordan

<sup>3</sup>Department of Electrical Engineering, Faculty of Engineering, Al-Hussein Bin Talal University, Maan, Jordan

<sup>4</sup>Department of Physics, Saber Faculty of Science and Education, University of Lahej, Lahej, Yemen

## Article Info

### Article history:

Received Jun 24, 2024

Revised Sep 10, 2024

Accepted Oct 1, 2024

### Keywords:

Harmonic impedance

Harmonics

Network modeling

Power system

Series and parallel resonances

## ABSTRACT

Since power systems are designed to work at the fundamental frequency, the presence of other frequencies from various sources may induce series and parallel resonances, leading to damage. The behavior of the power system in the presence of harmonics becomes evident with knowledge of harmonic impedance. Measurement offers the most accurate means of estimating harmonic impedance. However, when precise data of the power system parameters are available, highly satisfactory results can be achieved through calculation methods, particularly regarding loads, which are unknown and always change. This paper presents a study on estimating harmonic impedance using the Electromagnetic Transients Program Alternative Transient Program Draw (EMTP-ATPDraw) program, applied to an authentic network of Petrovice line 67, 22/0.4 kV, located in the Czech Republic. Hypothetically, the network was subjected to harmonic injection from a source (3<sup>rd</sup>, 5<sup>th</sup>, 7<sup>th</sup>, 9<sup>th</sup>, and 11<sup>th</sup> harmonics), and the harmonic impedance was calculated for three different variants: individual harmonics, all harmonics, and all except the 9<sup>th</sup> harmonic. The results show that the presence of the 9<sup>th</sup> harmonic can lead to a parallel resonance. This study is the first to employ EMTP-ATPDraw for programming this network. It gives the possibility to create a network database for different operating conditions, offering an asset for future project planning.

This is an open access article under the [CC BY-SA](https://creativecommons.org/licenses/by-sa/4.0/) license.



## Corresponding Author:

Wael Fawzi Abu Shehab

Department of Electrical Engineering, Faculty of Engineering, Al-Hussein Bin Talal University

Maan 71111, Jordan

Email: waelabushehab@ahu.edu.jo

## 1. INTRODUCTION

It is known that the power system is constructed to work at the fundamental frequency of 50 Hz (or 60 Hz), at which the power system has an impedance with an inductive character. Typically, the impedance combines source, transformer, transmission, and cable impedances. When a non-linear load injects harmonic currents into a power system, the system's impedance induces a voltage drop at each harmonic frequency. Consequently, the total harmonic voltage distortion at the terminals of a non-linear load equals the sum of these voltage drops [1]. Due to presence of frequencies other than the fundamental, parallel, and series resonances may occur due to the influence of power factor correction capacitors and cable capacities [2], [3], which may damage overvoltage or overcurrent conditions. It is noteworthy that most harmonic resonance issues are self-correcting. This implies that when the resonant condition occurs, it causes

sufficient currents or voltages within the system to either blow fuses, cause capacitor failure, or induce other damages that disrupt the system's resonance. The contrast between series and parallel resonance is that series resonance produces a low impedance, which draws maximum current into the system. In contrast, parallel resonance leads to high impedance, which causes significant harmonic voltage drop even with minimal current present and consequently results in damages associated with voltage stress.

Harmonic sources within the power system included transformer saturation [4], [5], industrial arc furnaces [6], and other arc devices such as large electric welders [7]. The rising prevalence of non-linear loads increases the harmonic distortion in the network. These loads include power converters employed in industrial applications (such as paper and steel industries, petrochemical industries, transportation industries, and food industries), multipurpose motor speed control systems, and various electric appliances [8], [9]. Various methods have been utilized for harmonic analysis, differing in modeling complexity, algorithms employed, and data prerequisites [10]–[15].

Harmonic currents typically characterize non-linear loads. Therefore, converting these harmonic currents into harmonic voltages is essential to determine the harmonic impedance. Knowledge of the harmonic impedance of the power system provides insight into how the system behaves for different harmonics. The relationship between network impedance and frequency is referred to as the harmonic impedance (or frequency characteristic) of the power system ( $Z = F(f)$ ). While measuring methods provide the most accurate estimation of harmonic impedance, calculating methods also yield satisfactory results [16]–[19].

Several techniques have been employed recently to estimate the harmonic impedance of the system, including Burg algorithm and autoregressive model [16], Kalman filter algorithm [17], Norton model and its improved circuit model [12], [18], a difference recurrence estimation method [19], Bayesian optimized Gaussian process regression [20], and improved rank regression method [21]. However, when a detailed knowledge of the electrical system is accessible and obtainable, the methods mentioned could be considered as intricate. In this study, a harmonic injection into a real known network is used to estimate the harmonic impedance of the system. In our case, this approach is regarded as less complicated compared to the methods outlined. The main contributions of this study are: i) Its ability to convert the real network into numerical data for software compatibility. To ensure successful simulation and accurate harmonic analysis, the network model components must be carefully chosen based on the analyzed problem; ii) Its capacity to establish a database of the power system for different variants. This database is valuable for planning new projects or integrating and installing new equipment within the system. Thus, knowing if the new changes will not disturb the power system will be easy; and iii) It can result in significant time and cost savings compared to measuring methods. To achieve the objectives of this study, the Electromagnetic Transients Program Alternative Transient Program Draw (EMTP-ATPDraw) program has been used, which is the graphical preprocessor for the alternative transient program (ATP) version of the electromagnetic transients program (EMTP) [22].

The subsequent sections of the paper are arranged as follows: The investigated network is described in section 2. Network construction and modeling is detailed in section 3. Section 4 discusses the simulation results. Finally, section 5 provides the conclusion of the paper.

## 2. DESCRIPTION OF THE INVESTIGATED NETWORK

The network of Petrovice-line 67, 22/0.4 kV, located in the Czech Republic, has a town distribution network character. The network comprises 17 distribution transformers with rated powers of 160, 250, and 400 kVA. The connection from the substation is realized by a 3×240 ANKTOY-PV cable (length 2.965 km), and it continues as an overhead line of 110 or 120 AlFe6 with branches of 70 AlFe6. The schema illustrating this network is depicted in Figure 1.

The primary challenge in modeling such networks lies in ensuring the accuracy of the values of the network components, especially the loads and the compensation powers, which are constantly changing, and the harmonic content generated by most of these loads. The problem arises when the calculation results must be compared to those obtained through measurements. Hence, several calculation variants need to be performed based on practical insights. These variants revolve around various operational scenarios and compensation power. Considering that the load value at each transformer is unknown, this study will consider 100% of the transformer-rated power with a power factor of  $\cos \alpha = 0.75$ .

Additionally, the compensation power will be considered to compensate from  $\cos \alpha = 0.75$  up to  $\cos \alpha_c = 0.98$ . The harmonic content will be assumed as a source that generates 3<sup>rd</sup>, 5<sup>th</sup>, 7<sup>th</sup>, 9<sup>th</sup>, and 11<sup>th</sup> harmonic currents, and it can be connected to any transformer within the network. The connection at the middle of the network (point 5064, transformer 160 kVA) will be sufficient for harmonic impedance estimation for three variants of harmonic content. The harmonic propagation in the network is depicted by the EMTP-ATPDraw simulation, and the resulting currents and voltages are visualized by PlotXY software

[23]. Moreover, PlotXY provides Fourier transformation for voltage and current, which can be used for impedance calculation. We are concerned with finding out the distorted voltage and current waveforms directly at the supply network Petrovice and subsequently determining the harmonic impedance.

### 3. CONSTRUCTION AND MODELLING OF THE NETWORK

The Petrovice network shown in Figure 1 is represented as a voltage source with internal impedance  $Z = R + jX$ , where  $R$  and  $X$  are resistance and reactance, respectively, calculated from the short-circuit power  $S_k''=1000$  MVA. The voltage amplitude  $V_{amp}$  and the system equivalent are calculated using (1), (2), and (3) [24], [25]:

$$V_{amp} = \sqrt{2} \times \frac{V}{\sqrt{3}}, \quad Y_{connected} \tag{1}$$

$$Z = c \cdot \frac{U_n^2}{S_k''}, \quad c = 1.1 \tag{2}$$

$$Z^2 = R^2 + (X_L)^2 = R^2 + (10R)^2, \quad X_L = j\omega L \tag{3}$$

$U_n, X_L, \omega, c,$  and  $L$  are nominal voltage in volts, inductive reactance in ohms, angular velocity in radians per second, voltage factor, and inductance in Henry, respectively. According to the investigated network, the voltage  $V$  in (1) is substituted with 22 kV.

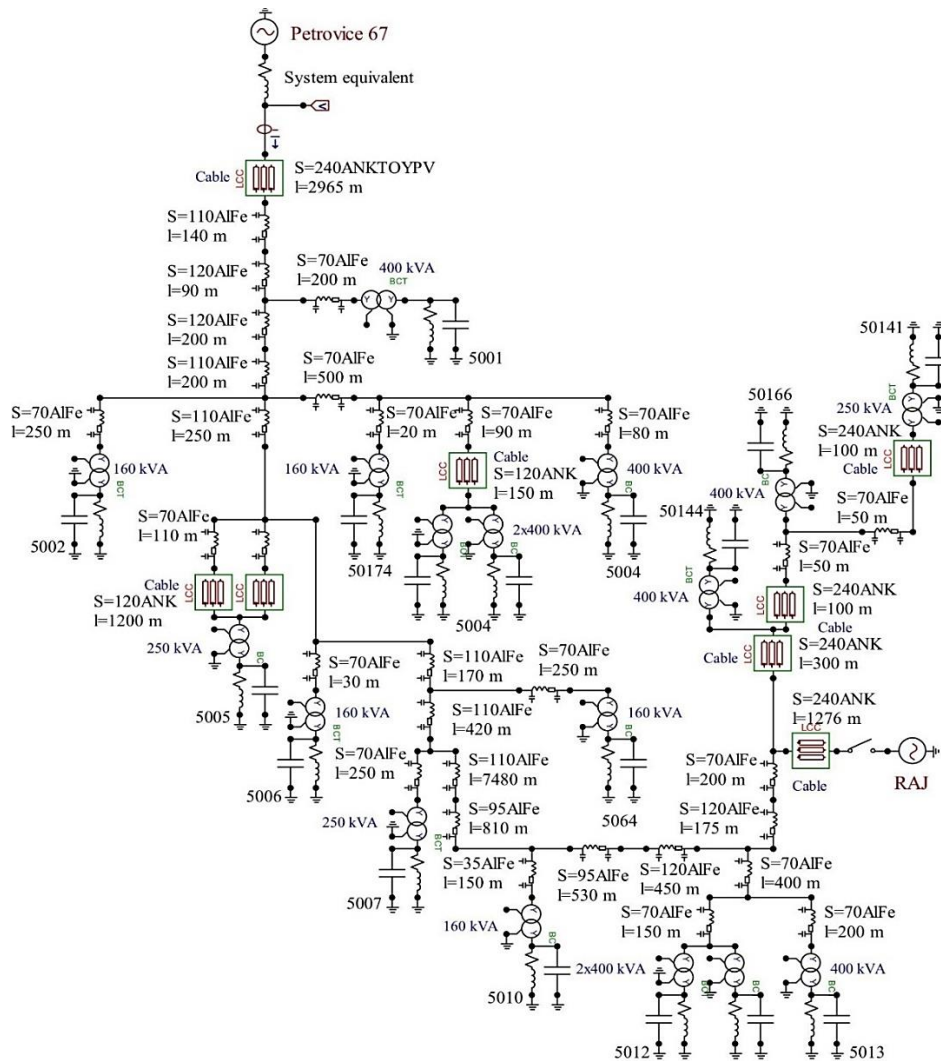


Figure 1. The investigated network constructed by EMTP-ATPDraw

The supply network can be modeled in the EMTP-ATPDraw using the ACSOURCE model (as a voltage source, single phase). Its parameters are listed in Table 1. Since the data of the distribution transformers are well known, they can be modeled by the BCTRAN model (as 1-phase, 1 W connected with earthed secondary) or by the SATTRAFO model since it consists of simple series R and L components [9]. Table 2 lists the parameters of the transformers.

Table 1. Parameters of the supply network

$V_{amp}$ (kV)	Z ( $\Omega$ )	R ( $\Omega$ )	L (mH)
17.963	0.532	0.053	1.687

Table 2. Parameters of the transformers

Power (kVA)	Short-circuit voltage (%)	Open-circuit current (%)	Short-circuit losses (kW)	Open-circuit losses (kW)
400	6	5.6	8.51	2
250	4.2	5.9	5.6	1.53
160	4.2	6.5	3.9	1.1

The resistance R and reactance X can represent cables and transmission lines. These values can be obtained either from manufacturer catalogs or through calculation. Several cable and transmission line models are available in the EMTP-ATPDraw, which can be easily implemented using the RLC parameters or the built-in procedure lines/cable (LCC). According to the available data, cable ANKTOY-PV can be modeled by the LCC JMarti model (1 phase, grounded,  $\rho=100 \Omega\text{m}$ ), as shown in Table 3. Concerning the transmission lines, the manufacturer provides the data for the transmission line AlFe6, as shown in Table 4. Hence, it will be easily modeled by the LINEPI\_1 model using RLC components.

Table 3. Parameters of the cable

Cross section ( $\text{mm}^2$ )	Inner radius $R_{in}$ (m)	Outer radius $R_{out}$ (m)	Material resistivity $\rho$ ( $\Omega\text{m}$ )	Material relative permeability $\mu$	Insulator relative permeability $\mu_u$	Insulator relative permittivity $\epsilon$
240	0.0093	0.0153	2.3E-8	1	1	2.3
120	0.00618	0.01225	2.3E-8	1	1	2.3

Table 4. Parameters of the transmission line

Cross section ( $\text{mm}^2$ )	R ( $\Omega/\text{km}$ )	L (mH/km)	C (nF/km)
120	0.250	1.064	10.950
110	0.259	1.077	10.806
70	0.429	1.124	10.331

As mentioned, the load will be considered 100% of the transformer-rated power with  $\cos \alpha = 0.75$ , and the power factor will be compensated to  $\cos \alpha_c = 0.98$ . RLC components can model the load without capacitance C, whereas C will be modeled separately from the compensational reactive power. The values of the loads are listed in Table 5 and calculated using (4), (5), and (6) [12], [26],

$$R = \frac{U^2}{P} \quad (4)$$

$$L = \frac{U^2}{2\pi f Q} \quad (5)$$

$$C = \frac{Q_C}{2\pi f U^2} \quad (6)$$

where S is the transformer-rated power in volt-ampere.

Although the harmonic content is typically acquired through measurement, for illustrative purposes, the harmonic source in the examined network is modeled by the HFS\_Sour model (harmonic frequency scan source, type 14), which injects the 3<sup>rd</sup>, 5<sup>th</sup>, 7<sup>th</sup>, 9<sup>th</sup>, and 11<sup>th</sup> harmonic currents to the network with hypothetical values provided in Table 6 for three calculation variants.

Table 5. Parameters of the loads

Transformer power S (kVA)	Cos $\alpha$	P (MW)	Q (MVar)	R ( $\Omega$ )	L (mH)	Q <sub>c</sub> (MVar)	C ( $\mu$ F)
400	0.75	0.300	0.265	0.53	1.93	0.204	4053.693
250		0.188	0.165	0.85	3.08	0.127	2533.558
160		0.120	0.106	1.33	4.81	0.081	1621.477

Table 6. The values of the harmonic currents

Harmonic order		3	5	7	9	11
Current (A)	Individual	200	200	200	200	200
	All	200	200	200	200	200
	All without 9 <sup>th</sup>	200	200	200	-	200

#### 4. RESULTS AND DISCUSSION

The network of Petrovice-line 67, shown in Figure 1, was constructed with one variant of the harmonic source connection and three variants of harmonic content, as described below:

- All loads in Table 5 were chosen as 100% of the transformer-rated power and were represented as RL components.
- Compensational capacitors were connected to all loads in Table 5 to compensate for the power factor from  $\cos \alpha = 0.75$  up to  $\cos \alpha_c = 0.98$ .
- The harmonic source in Table 6 was connected in the middle of the network (point 5064, transformer 160 kVA).
- The harmonic impedance was calculated from the voltage and current obtained directly from the Petrovice supply network.

The simulation by EMTP-ATPDraw yields distorted voltage and current curves observed within the supply network. The required next step that the PlotXY software offers is to perform Fourier transformation for the voltage and current as listed in Tables 7, 8, 9, and 10 for the three calculation variants, as follows:

- For individual harmonics as shown in Tables 7 and 8.
- For all harmonics as shown in Tables 9 and 10.
- For all harmonics without the 9<sup>th</sup> harmonic as shown in Tables 9 and 10.

Table 7. The harmonic voltages for variant 1

h	Magnitude (V)					h	Magnitude (V)				
	3 <sup>rd</sup>	5 <sup>th</sup>	7 <sup>th</sup>	9 <sup>th</sup>	11 <sup>th</sup>		3 <sup>rd</sup>	5 <sup>th</sup>	7 <sup>th</sup>	9 <sup>th</sup>	11 <sup>th</sup>
1	18396	18396.1	18396.1	18396.1	18396.1	11	0.05	0.03	0.03	0.10	948.19
2	0.50	0.62	0.61	0.58	0.60	12	0.05	0.03	0.02	0.06	0.54
3	1646.77	0.24	0.23	0.19	0.23	13	0.04	0.02	0.02	0.05	0.29
4	0.37	0.13	0.12	0.08	0.13	14	0.04	0.02	0.02	0.04	0.20
5	0.20	441.15	0.07	0.03	0.09	15	0.03	0.02	0.01	0.04	0.15
6	0.13	0.14	0.07	0.03	0.09	16	0.03	0.02	0.01	0.03	0.13
7	0.10	0.08	201.94	0.07	0.11	17	0.03	0.02	0.01	0.02	0.11
8	0.08	0.06	0.09	0.16	0.15	18	0.03	0.02	0.02	0.03	0.10
9	0.08	0.06	0.06	403.79	0.23	19	0.03	0.01	0.01	0.02	0.08
10	0.06	0.04	0.04	0.20	0.50	20	0.03	0.01	0.01	0.02	0.08

Table 8. The harmonic currents for variant 1

h	Magnitude (A)					h	Magnitude (A)				
	3 <sup>rd</sup>	5 <sup>th</sup>	7 <sup>th</sup>	9 <sup>th</sup>	11 <sup>th</sup>		3 <sup>rd</sup>	5 <sup>th</sup>	7 <sup>th</sup>	9 <sup>th</sup>	11 <sup>th</sup>
1	819.75	819.76	819.76	819.76	819.76	11	0.02	0.01	0.01	0.03	162.63
2	0.18	0.06	0.05	0.05	0.06	12	0.02	0.01	0.01	0.02	0.09
3	1035.07	0.04	0.03	0.03	0.04	13	0.02	0.01	0.01	0.02	0.04
4	0.18	0.05	0.02	0.02	0.03	14	0.02	0.01	0.01	0.01	0.03
5	0.09	166.43	0.02	0.01	0.03	15	0.02	0.01	0.01	0.01	0.02
6	0.06	0.04	0.02	0.01	0.03	16	0.02	0.01	0.01	0.01	0.02
7	0.04	0.02	54.43	0.01	0.03	17	0.01	0.01	0.01	0.01	0.01
8	0.04	0.02	0.02	0.03	0.04	18	0.01	0.01	0.01	0.01	0.01
9	0.03	0.01	0.02	84.65	0.05	19	0.01	0.01	0.00	0.01	0.01
10	0.03	0.01	0.01	0.05	0.09	20	0.01	0.01	0.00	0.01	0.01

These tables facilitate the calculation of harmonic impedance and the plotting of its curves. Tables 11 and 12 give the harmonic impedances for the three variants, while Figures 2, 3, and 4 display their

respective curves. The curves of the harmonic impedance for each harmonic in Figure 2 (variant 1) show the presence of resonances. The parallel resonance at the first harmonic (50 Hz) shows the inductive character of the network. The frequencies below 50 Hz values were neglected as they are irrelevant to our current focus. The parallel resonance due to the 9<sup>th</sup> harmonic clearly appears, which confirms the effect of the 9<sup>th</sup> harmonic on the harmonic impedance of the network with the given configuration. Next, the harmonic impedance was recalculated, considering the presence of all harmonics (variant 2), as depicted in Figure 3, where the curve illustrates the increase of the parallel resonance corresponding to the 9<sup>th</sup> harmonic. Upon recalculating the harmonic impedance without the 9<sup>th</sup> harmonic (variant 3), the parallel resonance corresponding to the 9<sup>th</sup> harmonic disappeared, as shown in Figure 4.

Table 9. The harmonic voltages for variants 2 and 3

h	Magnitude (V)		h	Magnitude (V)	
	Variant 2	Variant 3		Variant 2	Variant 3
1	18396.10	18396.00	11	948.14	948.19
2	0.43	0.47	12	0.52	0.54
3	1646.80	1646.84	13	0.26	0.28
4	0.45	0.48	14	0.18	0.19
5	440.93	440.91	15	0.14	0.15
6	0.10	0.14	16	0.11	0.12
7	201.85	201.82	17	0.09	0.10
8	0.12	0.11	18	0.08	0.09
9	403.90	0.23	19	0.07	0.08
10	0.61	0.49	20	0.06	0.07

Table 10. The harmonic currents for variants 2 and 3

h	Magnitude (V)		h	Magnitude (V)	
	Variant 2	Variant 3		Variant 2	Variant 3
1	819.75	819.75	11	162.62	162.63
2	0.14	0.14	12	0.09	0.09
3	1035.12	1035.12	13	0.05	0.05
4	0.22	0.23	14	0.04	0.03
5	166.36	166.35	15	0.03	0.03
6	0.05	0.06	16	0.03	0.02
7	54.41	54.40	17	0.02	0.02
8	0.01	0.04	18	0.02	0.02
9	84.69	0.05	19	0.02	0.02
10	0.12	0.10	20	0.02	0.02

Table 11. The harmonic impedances for variant 1

h	Magnitude ( $\Omega$ )					h	Magnitude ( $\Omega$ )				
	3 <sup>rd</sup>	5 <sup>th</sup>	7 <sup>th</sup>	9 <sup>th</sup>	11 <sup>th</sup>		3 <sup>rd</sup>	5 <sup>th</sup>	7 <sup>th</sup>	9 <sup>th</sup>	11 <sup>th</sup>
1	22.44	22.44	22.44	22.44	22.44	11	2.26	3.06	3.19	3.71	5.83
2	2.77	10.66	11.23	10.75	10.64	12	2.20	2.80	2.90	3.20	6.26
3	1.59	5.26	6.90	6.50	6.34	13	2.16	2.80	2.30	3.05	6.73
4	2.07	2.93	5.47	4.08	4.51	14	2.24	2.78	2.72	2.83	7.15
5	2.32	2.65	4.05	2.62	3.30	15	2.06	3.13	2.21	2.79	7.46
6	2.28	3.12	3.12	2.90	3.36	16	2.13	2.90	2.39	2.65	7.86
7	2.23	3.40	3.71	5.82	3.71	17	2.16	2.71	2.65	2.40	7.92
8	2.30	3.26	3.78	5.58	4.21	18	2.30	3.48	3.09	2.79	8.61
9	2.57	3.90	4.20	4.77	4.75	19	2.27	2.06	2.30	2.20	8.26
10	2.38	3.23	3.22	4.17	5.35	20	2.14	2.80	2.26	2.01	8.53

Table 12. The harmonic impedances for variants 2 and 3

h	Magnitude ( $\Omega$ )		h	Magnitude ( $\Omega$ )	
	Variant 2	Variant 3		Variant 2	Variant 3
1	22.44	22.44	11	5.83	5.83
2	3.07	3.50	12	5.72	5.94
3	1.59	1.59	13	5.15	5.97
4	2.01	2.08	14	4.79	5.64
5	2.65	2.65	15	4.34	5.45
6	1.90	2.21	16	4.07	5.33
7	3.71	3.71	17	3.67	4.96
8	17.18	2.43	18	3.69	4.97
9	4.77	4.11	19	3.24	4.57
10	4.87	5.18	20	3.20	4.47

As observed from these figures, the harmonic impedance of the network is influenced by both the composition and magnitudes of the harmonic currents injected into the network. Besides, it primarily relies on the configuration of the network. It is worth noting here that the total harmonic distortion (THD) can be computed using the PlotXY software. However, this step was not part of this study. The THD percentage must adhere to the standards outlined in the IEEE Std 519-2022 for harmonic limits [27]. The validation of the results in this study, which transforms the real electrical network into numerical data for software interpretation and processing, can be achieved by comparison with measurements. Unfortunately, these are not always possible due to the high cost associated with it. However, careful select of component models by trustworthy software is very important to understand the harmonic analysis and to success the simulation.

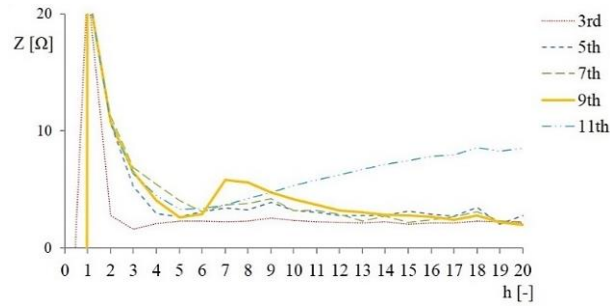


Figure 2. The harmonic impedance for variant 1

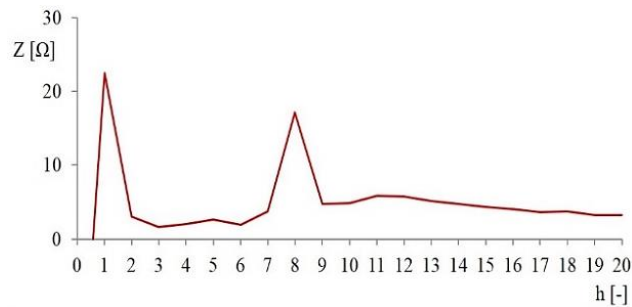


Figure 3. The harmonic impedance for variant 2

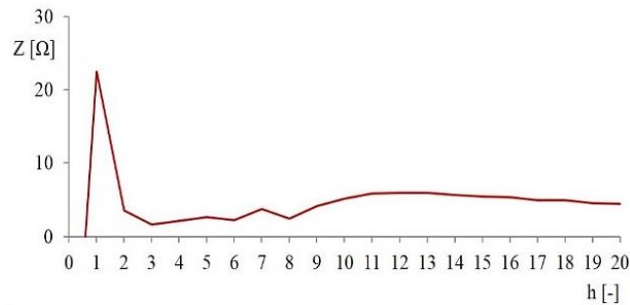


Figure 4. The harmonic impedance for variant 3

## 5. CONCLUSION

The study illustrates the capability of computer-based harmonic analysis to determine whether the system configuration is susceptible to drifting into series and parallel resonance conditions in the presence of harmonics. Moreover, the elements of the power system that exert an operational effect on harmonic impedance could be identified. The study has been confined to three calculation variants. However, there is potential to make changes in network elements to investigate harmonic impedance for different configurations or to identify the harmonic order responsible for resonance within a specified power system configuration. Our study shows that the 9<sup>th</sup> harmonic induces a parallel resonance in line 67, 22/0.4 kV branching from Petrovice. The challenge for calculation methods stems from the limited availability of load data for the network, even though data for other components can usually be obtained from manufacturer's catalogs. Such studies can aid in detailed analyses of specific power systems and in creating robust databases for electrical engineers and researchers to refine and advance their projects. Additionally, utilizing calculation methods can lead to substantial time and cost efficiencies compared to measurement approaches.




## REFERENCES

- [1] Ł. Michalec, M. Jasiński, T. Sikorski, Z. Leonowicz, Ł. Jasiński, and V. Suresh, "Impact of harmonic currents of nonlinear loads on power quality of a low voltage network-review and case study," *Energies*, vol. 14, no. 12, 2021, doi: 10.3390/en14123665.
- [2] S. Chaladying, P. Dusitakorn, and N. Rugthaichareoncheep, "Resonance impact on power factor correction system in

- power system with harmonic distortion,” *Applied Mechanics and Materials*, vol. 781, pp. 254–257, 2015, doi: 10.4028/www.scientific.net/amm.781.254.
- [3] Y. Yang and F. Blaabjerg, “Power factor correction capacitors for multiple parallel three-phase ASD systems: analysis and resonance damping,” in *2017 IEEE Energy Conversion Congress and Exposition, ECCE 2017*, 2017, vol. 2017-Janua, pp. 3398–3404, doi: 10.1109/ECCE.2017.8096609.
- [4] H. W. Dommel, A. Yan, and S. Wei, “Harmonics from transformer saturation,” *IEEE Transactions on Power Delivery*, vol. 1, no. 2, pp. 209–215, 1986, doi: 10.1109/TPWRD.1986.4307952.
- [5] I. Daut, S. Hasan, S. Taib, R. Chan, and M. Irwanto, “Harmonic content as the indicator of transformer core saturation,” in *PEOCO 2010 - 4th International Power Engineering and Optimization Conference, Program and Abstracts*, 2010, pp. 382–385, doi: 10.1109/PEOCO.2010.5559192.
- [6] Z. Olezykowski, “Arc voltage distortion as a source of higher harmonics generated by electric arc furnaces,” *Energies*, vol. 15, no. 10, 2022, doi: 10.3390/en15103628.
- [7] S. V. Rymar, A. M. Zhernosekov, and V. N. Sidorets, “Effect of single-phase power sources of welding arc on electric mains,” *The Paton Welding Journal*, no. November 2016, pp. 9–15, 2011.
- [8] F. C. De La Rosa, “Fundamentals of harmonic distortion and power quality indices in electric power systems,” *Harmonics and Power Systems*, pp. 19–44, 2020, doi: 10.1201/9781420004519-5.
- [9] S. A. Ali, “Modeling of power networks by ATP-Draw for harmonics propagation study,” *Transactions on Electrical and Electronic Materials*, vol. 14, no. 6, pp. 283–290, 2013, doi: 10.4313/TEEM.2013.14.6.283.
- [10] X. Xiao, R. Zhou, X. Ma, and R. Xu, “A novel method for estimating utility harmonic impedance based probabilistic evaluation,” *IET Generation, Transmission and Distribution*, vol. 16, no. 7, pp. 1438–1448, 2022, doi: 10.1049/gtd2.12380.
- [11] M. J. Ghorbani and H. Mokhtari, “Impact of harmonics on power quality and losses in power distribution systems,” *International Journal of Electrical and Computer Engineering*, vol. 5, no. 1, pp. 166–174, 2015, doi: 10.11591/ijece.v5i1.pp166-174.
- [12] M. I. Alsharari, M. Z. Ahmed, W. F. Abu Shehab, and S. A. Ali, “Evaluation of harmonic currents and network impedance using Norton model in an unidentified network configuration,” *Jordan Journal of Electrical Engineering*, vol. 10, no. 1, pp. 84–95, 2024, doi: 10.5455/jjee.204-1686253514.
- [13] J. Yong, L. Chen, A. B. Nassif, and W. Xu, “A frequency-domain harmonic model for compact fluorescent lamps,” *IEEE Transactions on Power Delivery*, vol. 25, no. 2, pp. 1182–1189, 2010, doi: 10.1109/TPWRD.2009.2032915.
- [14] M. H. Jopri, A. Skamyin, M. Manap, T. Sutikno, M. R. M. Shariff, and A. Belsky, “Identification of harmonic source location in power distribution network,” *International Journal of Power Electronics and Drive Systems*, vol. 13, no. 2, pp. 938–949, 2022, doi: 10.11591/ijpeds.v13.i2.pp938-949.
- [15] A. Skamyin, Y. Shklyarskiy, K. Lobko, V. Dobush, T. Sutikno, and M. H. Jopri, “Impedance analysis of squirrel-cage induction motor at high harmonics condition,” *Indonesian Journal of Electrical Engineering and Computer Science*, vol. 33, no. 1, pp. 31–41, 2024, doi: 10.11591/ijeecs.v33.i1.pp31-41.
- [16] Q. Shu, Y. Fan, F. Xu, C. Wang, and J. He, “A harmonic impedance estimation method based on AR model and Burg algorithm,” *Electric Power Systems Research*, vol. 202, 2022, doi: 10.1016/j.epr.2021.107568.
- [17] Z. Luo, B. Hou, and P. Zhao, “A method for estimating the harmonic impedance in real time based on Kalman filter algorithm,” *Journal of Physics: Conference Series*, vol. 2477, no. 1, 2023, doi: 10.1088/1742-6596/2477/1/012089.
- [18] H. Zheng, F. Xu, Q. Shu, C. Wang, and Q. Zhou, “Estimation of harmonic impedance and harmonic contribution with harmonic complex power in the absence of harmonic phase angle,” *IET Generation, Transmission and Distribution*, vol. 17, no. 1, pp. 200–208, 2023, doi: 10.1049/gtd2.12673.
- [19] H. Hua, H. Gao, L. Gao, and H. Guo, “A novel method for calculating harmonic contribution based on difference recurrence estimation,” *IET Generation, Transmission and Distribution*, vol. 18, no. 3, pp. 596–608, 2024, doi: 10.1049/gtd2.13097.
- [20] Y. Xia and W. Tang, “Study on the estimation of harmonic impedance based on Bayesian optimized Gaussian process regression,” *International Journal of Electrical Power and Energy Systems*, vol. 142, 2022, doi: 10.1016/j.ijepes.2022.108294.
- [21] D. Wang, J. Chen, Q. Yin, H. Ding, Q. Liu, and H. Miao, “Harmonic impedance estimation based on improved rank estimation,” *Journal of Physics: Conference Series*, vol. 2771, no. 1, 2024, doi: 10.1088/1742-6596/2771/1/012034.
- [22] H. Hoidalén, L. Prikler, and F. Penalzoza, “ATPDraw version 7.3 for Windows- users’ manual,” *Norwegian University of Science and Technology (NTNU)*, 2021.
- [23] M. Ceraolo, “MC’s PlotXY—A general-purpose plotting and post-processing open-source tool,” *SoftwareX*, vol. 9, pp. 282–287, Jan. 2019, doi: 10.1016/j.softx.2019.01.017.
- [24] J. Schlabbach, *Short circuit currents*. Institution of Engineering and Technology, 2005.
- [25] T. N. Boutsika and S. A. Papathanassiou, “Short-circuit calculations in networks with distributed generation,” *Electric Power Systems Research*, vol. 78, no. 7, pp. 1181–1191, Jul. 2008, doi: 10.1016/j.epr.2007.10.003.
- [26] S. A. Ali and A. Bodor, “Evaluation of the harmonic impedance of Frydlant (Line 53) power network,” *Advances in Electrical and Electronic Engineering*, vol. 11, no. 4, Sep. 2013, doi: 10.15598/aeec.v11i4.696.
- [27] IEEE, “IEEE standard for harmonic control in electric power systems,” *IEEE Std 519-2022 (Revision of IEEE Std 519-2014)*, pp. 1–31, 2022.




## BIOGRAPHIES OF AUTHORS






**Haitham Ali Alashaary**    received the B.S. degree in electronics engineering from the Yarmouk University, Irbid, Jordan, in 2000, the M.Sc. degree in biomedical engineering from the University of New South Wales, Australia, in 2003, and the Ph.D. degree in electrical and computer engineering from the University of Newcastle, Australia in 2010. He is currently an associate professor at Al-Hussein Bin Talal University, Jordan. His research interests include, but not limited to neural networks, fuzzy logic, neuro-fuzzy techniques, signal and image processing, automatic control, parallel computing, and electronics. He can be contacted at email: haitham.alashaary@ahu.edu.jo.








**Ghadeer Nyazi Al Shaba'an**    received the B.Sc. degree in electronic engineering, from the Princess Sumaya University for Technology, Amman, Jordan, in 2004. She received the M.Sc. and Ph.D. degrees in electronic engineering from School of Engineering and Physical Science, University of Dundee, UK, in 2005 and 2010, respectively. She is currently an associate professor at the Department of Electrical Engineering, Al-Balqa Applied University, Jordan. Her research interests include electronics and renewable energy systems. She can be contacted at email: ghadeer.sh@bau.edu.jo.



**Wael Fawzi Abu Shehab**    received the M.Sc. and Ph.D. degrees in electronics and telecommunication technique from VSB-Technical University of Ostrava, Czech Republic, in 1997 and 2001, respectively. From 2001 to 2009, he was a lecturer and the head of the Department of Industrial Electronics and Control at Jazan College of Technology, Saudi Arabia. Since 2010, he has been with Al-Hussein Bin Talal University at Ma'an, Jordan, where he is currently a professor at the Department of Electrical Engineering. His research interest spans a wide range of topics including electrical networks, optical fiber sensors and wireless communications. He can be contacted at email: waelabushehab@ahu.edu.jo.



**Shehab Abdulwadood Ali**    received the M.Sc. and Ph.D. degrees in the field of Electrical Power Engineering from VSB-Technical University of Ostrava, Czech Republic, in 1993 and 2002, respectively. He is currently a Professor at the Department of Physics, Saber Faculty of Science and Education, University of Lahej, Yemen. His research interests include, but not limited to, power quality and electromagnetic compatibility problems with using ATPDraw and NetCalc. He can be contacted at email: shehababdulwadood@gmail.com.